JOURNAL OF AIRCRAFT
Vol. 39, No. 2, March–April 2002

Strength of 7075-T6 and 2024-T3 Aluminum Panels with Multiple-Site Damage

B. L. Smith,* A. L. Hijazi,† and R. Y. Myose‡
Wichita State University, Wichita, Kansas 67260-0044

Much attention has been given to the development of technology for the purpose of determining the strength of aluminum panels that have multiple-site damage. The linkup model has been investigated because of its simplicity, and a number of modified linkup models have been presented. However, most of the attention has been given to 2024-T3 aluminum. Little attention has been given to 7075-T6 because it is a more brittle material with lower fracture toughness, making it more suitable to be analyzed by conventional linear elastic (brittle) fracture mechanics technology. The work presented here involves the study of 7075-T6 panels with multiple-site damage. Both the classical linear elastic fracture model and the linkup model are shown to be highly inaccurate. A modified linkup model and a modified brittle fracture model have both been developed by empirical analysis. Both of these models appear to have a high degree of accuracy over a wide range of crack geometry. The modified linkup model for 7075-T6 is then compared with a previously developed modified linkup model for 2024-T3. This comparison shows that 2024-T3 panels with multiple-site damage have greater strength than 7075-T6 panels, especially for panels with small ligament lengths.

Nomenclature

a	=	lead crack half-length
a_n	=	nominal lead crack half-length
c	=	multiple-site damage (MSD) crack length
D	=	hole diameter
K_c	=	apparent fracture toughness
L	=	ligament length
ℓ	=	half-length for MSD crack and hole, $c + D/2$
R	=	ratio of critical strength of 2024 to 7075
W	=	panel width
β_a	=	correction to stress intensity of the lead crack, $\beta_{a/\ell}\beta_W$
$\beta_{a/\ell}$	=	correction to stress intensity of the lead crack for the effect of the adjacent MSD crack
β_b	=	correction to stress intensity of the adjacent MSD crack for the effect of an open hole
β_ℓ	=	correction to stress intensity of the adjacent MSD crack, $\beta_{\ell/a}\beta_b\sqrt{(c/\ell)}$
$\beta_{\ell/a}$	=	correction to stress intensity of the adjacent MSD crack for the effect of the lead crack
β_W	=	finite width correction to stress intensity of the lead crack
σ_{bf}	=	critical stress for ligament failure based on brittle fracture
$\sigma_{\text{bf,mod(7075)}}$	=	critical stress for ligament failure based on modified brittle fracture for 7075-T6
σ_c	=	critical stress for ligament failure
σ_{lu}	=	critical stress for ligament failure based on linkup
$\sigma_{\text{lu,mod(7075)}}$	=	critical stress for ligament failure based on modified linkup for 7075-T6
σ_{test}	=	critical stress for ligament failure based on testing
$\sigma_{\text{wsu2(2024)}}$	=	critical stress for ligament failure based on modified linkup for 2024-T3
σ_{ys}	=	yield strength

Introduction

MUCH attention has been given to the remote stress corresponding to ligament failure for 2024-T3 aluminum panels with multiple-site damage (MSD). A schematic diagram of such a panel is shown in Fig. 1. It has a central lead crack of length $2a$ and collinear (MSD) cracks emerging from the adjacent holes. The small-scale cracking referred to as MSD occurs in aging aircraft as a result of fatigue loading. A value of the remote stress that produces crack extension and ligament failure is referred to herein as a critical stress. This critical stress cannot be determined with conventional brittle fracture based on fracture toughness. In an attempt to explain this phenomenon, Swift[1] described an analytical model called the linkup model or the plastic zone touch model. The linkup model clearly shows the adverse effect of MSD; however, it does not accurately predict the magnitude of the remote stress corresponding to ligament failure for many geometric configurations. A number of different modifications of the linkup model have been developed.[2–4] Smith et al.[4] developed two modified linkup models, one being a nondimensionalized version of the other. These models were developed by empirical analysis based on test data from 40 different unstiffened panels and later validated with test data from 36 different stiffened panels.[5] All of these models were developed only for 2024-T3 aluminum because this is the primary material used in aircraft skin. However, an important material still in use, but to a lesser extent, is 7075-T6 aluminum. Thus, a question arose as to the behavior of 7075-T6 panels with MSD.

The purpose of the project described herein was to develop an analytical model for 7075-T6 and then to compare the remote stress that produces ligament failure in 2024-T3 with that of 7075-T6. Two analytical models were developed by empirical analyses based on test data from panels with 12 different crack configurations. One of these models is a modified linkup model that requires the use of yield stress, and the other model is a modified brittle fracture model that requires the use of fracture toughness. The modified linkup model for 7075-T6 developed and described herein and the linkup model previously developed[4] for 2024-T3 were then used to compare the remote stresses corresponding to ligament failure for these two materials.

Received 27 June 2001; revision received 25 September 2001; accepted for publication 10 December 2001.

*Professor, Department of Aerospace Engineering. Senior Member AIAA.

†Graduate Research Assistant, Department of Aerospace Engineering.

‡Associate Professor, Department of Aerospace Engineering. Associate Fellow AIAA.

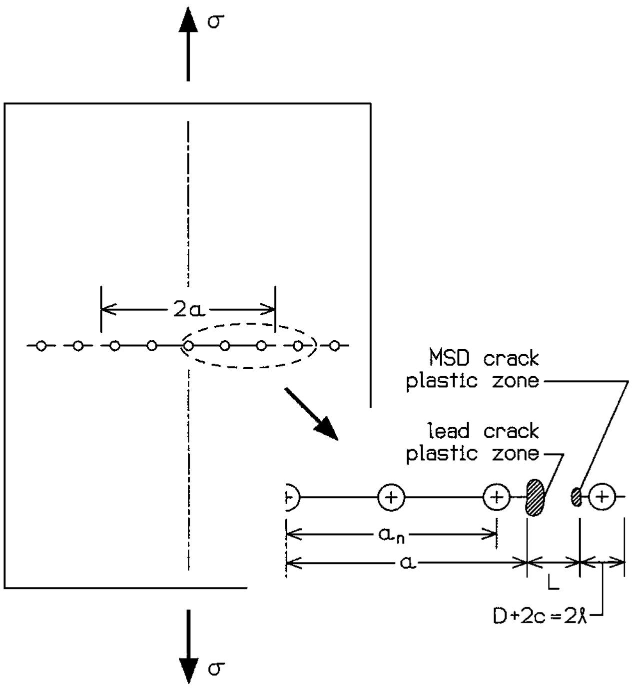

Fig. 1 Schematic diagram of panel with MSD.

Linkup Model

The analytical model, described by Swift[1] and first used to predict the value of the remote stress corresponding to ligament failure, is often referred to as the linkup model or the plastic zone touch model and is given in Eq. (1), as follows:

$$\sigma_{\text{lu}} = \sigma_{\text{ys}}\sqrt{2L\big/\left(a\beta_a^2 + \ell\beta_\ell^2\right)} \tag{1}$$

The corrections to stress intensity of the lead crack and adjacent MSD crack (Fig. 1) are as follows.

Lead crack:

$$\beta_a = \beta_{a/\ell}\beta_W \tag{2}$$

Adjacent crack:

$$\beta_\ell = \beta_{\ell/a}\beta_b\sqrt{c/\ell} \tag{3}$$

The correction to the stress intensity of the lead crack for the effect of the adjacent MSD crack is $\beta_{a/\ell}$ (Ref. 6, p. 119), and β_W is the finite width correction to stress intensity of the lead crack and is given by $\beta_W = \sqrt{[\sec(\pi a/W)]}$. The correction to the stress intensity of the adjacent MSD crack for the effect of the lead crack is $\beta_{\ell/a}$ (Ref. 6, p. 117), and β_b is the correction for open holes (Ref. 7), which is given by the following equation:

$$\beta_b = 1 - \frac{0.15}{1+2c/D} + \frac{3.46}{(1+2c/D)^2} - \frac{4.47}{(1+2c/D)^3} + \frac{3.52}{(1+2c/D)^4} \tag{4}$$

Equation (1) is based on the concept that ligament failure will occur when the remote stress σ reaches a level that causes the surfaces of the lead crack tip plastic zone and the adjacent MSD crack tip plastic zone (Fig. 1) to touch. Unfortunately, the linkup model has proven to be unreliable, as previously shown.[4] It is accurate for some configurations, but highly inaccurate for others. Thus, the modified models[2–4] have been developed.

Modified Linkup Model for 2024-T3

A modified linkup model developed by Smith et al.[4] for 2024-T3 and used later to compare the two materials 2024-T3 and 7075-T6 is given in Eq. (5). This model was referred to as the WSU2 model in Ref. 4, and that designation will be used here,

$$\sigma_{\text{wsu2(2024)}} = \frac{\sigma_{\text{lu}}}{C_1 \ln(L) + C_2} \tag{5}$$

In Eq. (5) the stresses σ are in units of ksi, and the ligament length L is in inches. The coefficients C_1 and C_2 were determined from an empirical analysis based on MIL-HDBK-5G yield strength values. For A-basis yield strength values, the coefficients are $C_1 = 0.3065$ and $C_2 = 1.3123$. For B-basis yield strength values, the coefficients are $C_1 = 0.3054$ and $C_2 = 1.3502$. A nondimensionalized version of Eq. (5) was also presented; however, it was slightly less accurate, and, therefore, it is not used here.

Test Data for the 7075-T6 Panels

A servohydraulic testing machine was used to obtain the loads required to produce ligament failure for the 7075-T6 panels. Figure 2 shows a test panel along with test fixturing. The panels were 24 in. wide and 36 in. long, and the holes along the crack line were 0.25 in. in diameter with a pitch of 1 in. Midspan fixtures were used to prevent buckling along the crack line, and heavy stiffeners were used at each end to help distribute the load across the width. During earlier testing it was determined that the same results could be obtained by using either stroke or load control. Therefore, stroke control was used at a rate of 0.01 in./min. Real-time observations were made with a closed-circuit television system, which allowed magnified viewing of the lead crack and adjacent MSD crack. A charge-coupled device camera and super-video home system (S-VHS) video recorder recorded the observed test results. A time code generator imprinted a time reference on the video every $\frac{1}{30}$ of a second. This allowed frame-by-frame viewing of the recorded images and comparison against quantitative measurements of load vs time made by the servohydraulic test machine. The critical values of remote stress σ for ligament failure obtained from testing are designated as σ_{test} and given in Table 1 for each of the 12 panels.

The synthetic MSD cracks were produced by saw cut. During previous testing,[4] the synthetic MSD cracks were produced by both saw cut and electrodischarge machine (EDM) and found to give equivalent results. The cracks produced by EDM were more reliable; thus, duplicate testing for statistical accuracy was not necessary in the earlier testing. Because the EDM cracks had to be produced by an outside source, which was no longer available, the cracks were produced by saw cut. Only 12 panels were available for testing the 7075-T6 material. Although saw cuts are not as reliable as EDM notches, it was decided that 12 different configurations would be more useful than 6 different duplicate configurations or 4 different triplicate configurations. The 12 panels tested were bare (rather than clad), the load was applied perpendicular to the grain, and the panel thickness was 0.071 in. Thus, the A-basis and B-basis yield strengths were 68 and 70 ksi, respectively, according to MIL-HDBK-5G. Several panels were also tested for apparent fracture toughness (based on initial crack length), which was found to be 70 ksi (in.)$^{1/2}$. Details of the crack configuration for each of the 12 panels are given in Table 1.

Table 1 Crack geometry and experimental stresses (7075-T6)

Panel	a, in.	c, in.	L, in.	σ_{test}, ksi
1	3.325	0.15	0.40	14.59
2	4.325	0.20	0.35	11.75
3	4.275	0.15	0.45	13.67
4	4.275	0.10	0.50	14.06
5	4.225	0.05	0.60	15.28
6	5.275	0.10	0.50	11.78
7	5.225	0.10	0.55	13.12
8	5.325	0.15	0.40	10.91
9	6.225	0.10	0.55	11.21
10	7.525	0.20	0.15	4.73
11	7.475	0.20	0.20	5.98
12	7.425	0.20	0.25	6.77

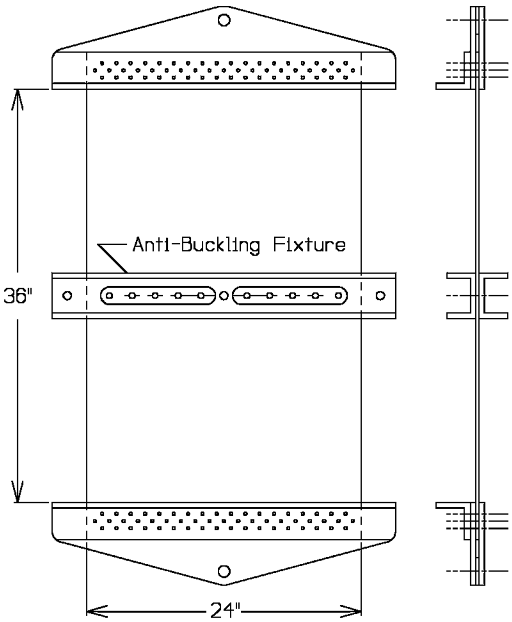

Front and side view schematic diagram of test setup

Photograph of actual test panel in the servohydraulic test machine

Fig. 2 Test setup.

Modified Brittle Fracture Model for 7075-T6

The critical value of remote stress based on brittle fracture is given in Eq. (6), as follows:

$$\sigma_{\mathrm{bf}} = K_c \Big/ \sqrt{\pi a}\,\beta_a \tag{6}$$

This equation predicts values for critical stress that are much too high; therefore, it becomes necessary to adjust or modify this equation so that it matches the test values. This modification is developed from the data as displayed in Fig. 3. The ligament length is plotted on the horizontal axis, whereas the difference between the brittle fracture stress σ_{bf} and the test value σ_{test} divided by the test value

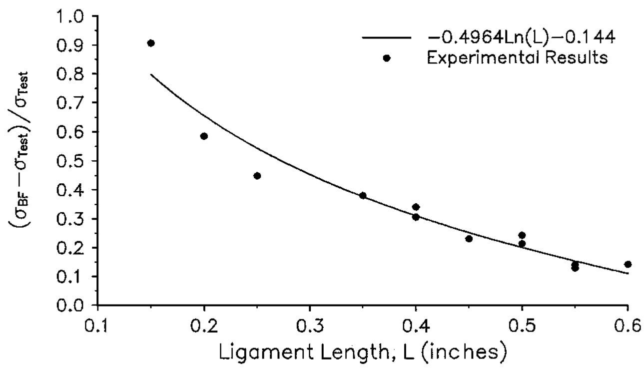

Fig. 3 Natural log form correction for modified brittle fracture model.

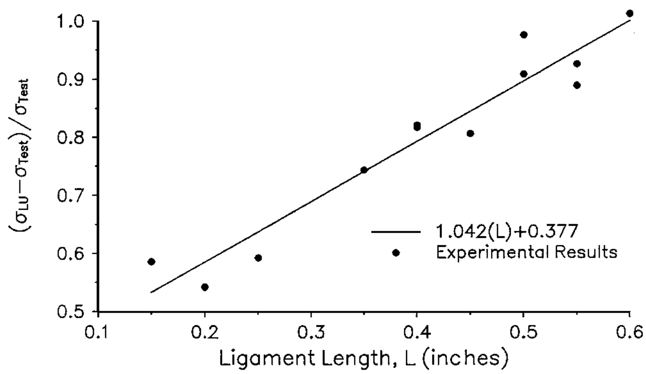

Fig. 4 Linear form correction for modified linkup model (for A-basis yield strengths).

is plotted on the vertical axis. Although there is some scatter in the data, a reasonably good representation of the data can be made with a single equation of the natural log form. When the data are represented by a single curve, the stress σ_{test} becomes the critical stress based on a modification of brittle fracture:

$$(\sigma_{\mathrm{bf}} - \sigma_c)/\sigma_c = -0.4964 \ln(L) - 0.144 \tag{7}$$

$$\sigma_c = \sigma_{\mathrm{bf}}/[0.856 - 0.4964 \ln(L)] \tag{8}$$

$$\sigma_c = K_c \Big/ \left\{\sqrt{\pi a}\,\beta_a[0.856 - 0.4964 \ln(L)]\right\} \tag{9}$$

or

$$\sigma_{\mathrm{bf,mod(7075)}} = K_c \Big/ \left\{\sqrt{\pi a}\,\beta_a[0.856 - 0.4964 \ln(L)]\right\} \tag{10}$$

Equation (10) is the expression for the critical stress based on a modification of the brittle fracture equation, which was developed from empirical analysis described earlier.

Modified Linkup Model for 7075-T6

The critical stress based on linkup, given in Eq. (1), also predicts values that are much too high; therefore, it also becomes necessary to modify this equation so that it matches the test values. This modification is developed from the data as displayed in Fig. 4 for the A-basis yield strengths. The corresponding curve for the B-basis yield strengths is not shown, but is similar. The ligament length is plotted on the horizontal axis, whereas the difference between the linkup stress σ_{lu} and the test value σ_{test} divided by the test value is plotted on the vertical axis. Although there is some scatter in the data, a reasonably good representation of the data can be made with a single linear equation. When the data are represented by a single curve, the stress σ_{test} becomes the critical stress based on a modification of the linkup equation:

$$(\sigma_{\mathrm{lu}} - \sigma_c)/\sigma_c = D_1 L + D_2 \tag{11}$$

$$\sigma_c = \sigma_{\mathrm{lu}}/(D_1 L + D_2 + 1) \tag{12}$$

$$\sigma_c = \sigma_{\mathrm{lu}}/(D_1 L + D_3) \tag{13}$$

or

$$\sigma_{\mathrm{lu,Mod(7075)}} = \sigma_{\mathrm{lu}}/(D_1 L + D_3) \tag{14}$$

Equation (14) is the expression for the critical stress based on a modification of the linkup equation, which was developed from the empirical analysis described earlier. If A-basis yield strength values are used in Eq. (14), the coefficients are $D_1 = 1.042$ and $D_3 = 1.377$. If B-basis yield strength values are used, the coefficients are $D_1 = 1.073$ and $D_3 = 1.417$.

Results

The results based on brittle fracture, Eq. (6), and modified brittle fracture, Eq. (10), are given in Table 2. For each panel configuration, the absolute value of the difference between the test value and each of the analytical models was determined, then multiplied by 100 and defined as a percent error. The average error for the brittle fracture model is 33.86%, whereas that for the modified brittle fracture model is 2.65%. The brittle fracture model has predicted critical stresses that are too high for every panel. The results based on linkup, Eq. (1), and modified linkup, Eq. (14), are given in Tables 3 and 4. The results in Table 3 are based on A-basis yield strength values, whereas those in Table 4 are based on B-basis yield strength values. The values for $\sigma_{\mathrm{lu,mod}}$ for A-basis yield strengths are the same as those for B-basis yield strengths because the curve fit is linear. For the A-basis results, the average error is reduced from 80.21% for the linkup model to 1.97% for the modified linkup model. For the B-basis results, the average error is reduced from 85.51% for the linkup model to 1.97% for the modified linkup model. Also note that, although both unmodified models give poor results, the brittle fracture model yields more accurate results than the linkup model.

The ratio of the critical strengths of 2024-T3 to that of 7075-T6 can be investigated easily by dividing Eq. (5) by Eq. (14) and denoting the ratio by R:

$$R = \frac{\sigma_{\mathrm{wsu2(2024)}}}{\sigma_{\mathrm{lu,mod(7075)}}} = \frac{\sigma_{\mathrm{ys(2024)}}(D_1 L + D_3)}{\sigma_{\mathrm{ys(7075)}}[C_1 \ln(L) + C_2)} \tag{15}$$

Table 2 Critical stresses based on brittle fracture and modified brittle fracture (7075)

Panel	σ_{bf}, ksi	$\sigma_{\mathrm{bf,mod}}$, ksi	σ_{bf}, % error	$\sigma_{\mathrm{bf,mod}}$, % error
1	19.57	14.93	34.12	2.32
2	16.23	11.78	38.06	0.25
3	16.83	13.44	23.11	1.70
4	17.06	14.21	21.35	1.11
5	17.44	15.72	14.15	2.88
6	14.64	12.20	24.30	3.58
7	14.81	12.85	12.92	2.04
8	14.25	10.87	30.58	0.39
9	12.78	11.08	14.00	1.11
10	9.02	5.02	90.49	5.96
11	9.48	5.73	58.37	4.31
12	9.81	6.35	44.91	6.15
Average % error			33.86	2.65

Table 3 Critical stresses based on linkup and modified linkup for 7075 and A-basis yield strengths

Panel	σ_{lu}, ksi	$\sigma_{\mathrm{lu,mod}}$, ksi	σ_{lu}, % error	$\sigma_{\mathrm{lu,mod}}$, % error
1	26.58	14.82	82.22	1.60
2	20.49	11.77	74.35	0.13
3	24.70	13.38	80.70	2.09
4	26.85	14.15	91.02	0.66
5	30.77	15.37	101.38	0.59
6	23.29	12.27	97.66	4.16
7	24.80	12.72	89.07	3.03
8	19.83	11.06	81.75	1.34
9	21.60	11.08	92.73	1.16
10	7.50	4.89	58.45	3.37
11	9.22	5.82	54.06	2.80
12	10.78	6.58	59.18	2.76
Average % error			80.21	1.97

Table 4 Critical stresses based on linkup and modified linkup for 7075 and B-basis yield strengths

Panel	σ_{lu}, ksi	$\sigma_{\mathrm{lu,mod}}$, ksi	σ_{lu}, % error	$\sigma_{\mathrm{lu,mod}}$, % error
1	27.37	14.82	87.58	1.60
2	21.10	11.77	79.48	0.13
3	25.42	13.38	86.02	2.09
4	27.64	14.15	96.63	0.66
5	31.68	15.37	107.3	0.59
6	23.97	12.27	103.5	4.16
7	25.53	12.72	94.63	3.03
8	20.41	11.06	87.09	1.34
9	22.24	11.08	98.40	1.15
10	7.72	4.89	63.11	3.37
11	9.49	5.82	58.59	2.80
12	11.10	6.58	63.87	2.76
Average % error			85.51	1.97

Table 5 Ratio of critical stress of 2024-T3 to 7075-T6 [Eq. (15)]

L, in.	R
0.15	1.312
0.20	1.210
0.25	1.154
0.30	1.120
0.40	1.087
0.50	1.079
0.65	1.083
0.70	1.095
0.75	1.102

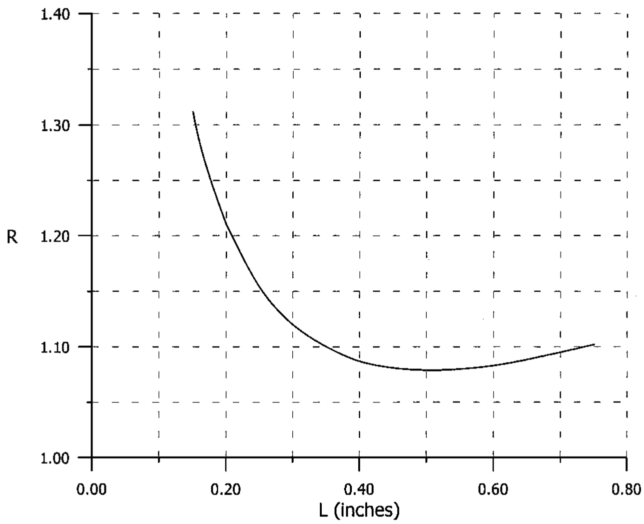

Fig. 5 Ratio of the critical stress of 2024-T3 to that of 7075-T6.

For a numerical comparison, an example is shown based on the following two materials from MIL-HDBK-5G: For 2024-T3, $t = 0.071$ in., clad, long-transverse (LT) grain direction, A-basis, and $\sigma_{\mathrm{ys}} = 40$ ksi; for 7075-T6, $t = 0.071$ in., clad, LT grain direction, A-basis, and $\sigma_{\mathrm{ys}} = 64$ ksi.

Based on this information, the values of R are determined for various ligament lengths, and the results are shown in Table 5 and plotted in Fig. 5. Figure 5 shows that the critical strength of 2024-T3 is greater than that of 7075-T6 for all ligament lengths. However, it is significantly higher as the ligament length decreases.

Conclusions

The critical strength of 7075-T6 aluminum panels with MSD cannot be predicted accurately with either the conventional brittle fracture method or the linkup equation. This is especially important because 7075-T6 is a rather brittle material that might be expected to behave according to linear elastic fracture methodology. However, it was shown that the brittle fracture model gave better results than the linkup model, which is the opposite for 2024-T3. With testing over a wide range of ligament lengths followed by an empirical analysis, it was shown that a modified brittle fracture model and a modified linkup model both appear to give very good results. Smith et al. showed that a modified linkup model developed from open-hole unstiffened panels for 2024-T3 aluminum could be used for a variety of panel configurations including several different kinds of stiffened panels. There is no reason to believe that the same is not true for 7075-T6. The critical strength of 2024-T3 appears to be greater than 7075-T6 panels with MSD, especially for small ligament lengths. The results of this investigation show a difference in residual strength between 2024-T3 and 7075-T6; however, note that the results were based on a limited number of test configurations for the 7075-T6 material.

Acknowledgments

This work was sponsored by the industrial members of the Aircraft Design and Manufacturing Research Center of Wichita State University, Wichita, Kansas. The material for the aluminum panels was donated by Lockheed Martin Aeronautical Systems, Marrietta, Georgia.

References

[1]Swift, T., "Widespread Fatigue Damage Monitoring Issues and Concerns," 5th International Conf. on Structural Airworthiness of New and Aging Aircraft, June 1993.

[2]Broek, D., "The Effects of Multi-Site Damage on the Arrest Capability of Aircraft Fuselage Structure," FractuResearch TR 9302, Galena, OH, June 1993.

[3]Ingram, J. E., Kwon, Y. S., Duffie, K. J., and Irby, W. D., "Residual Strength Analysis of Skin Splices with Multiple Site Damage," Proceedings of the 2nd Joint NASA/FAA/DoD Conference on Aging Aircraft, edited by Charles Harris, NASA Langley Research Center, Hampton, VA, NASA CP-1999-208982.

[4]Smith, B., Saville, P., Mouak, A., and Myose, R., "Strength of 2024-T3 Aluminum Panels with Multiple Site Damage," *Journal of Aircraft*, Vol. 37, No. 2, 2000, pp. 325–331.

[5]Smith, B. L., Hijazi, A. L., Haque, A. K. M., and Myose, R., "Strength of Stiffened 2024-T3 Aluminum Panels with Multiple Site Damage," *Journal of Aircraft*, Vol. 38, No. 4, 2001, pp. 764–768.

[6]Rooke, D. P., and Cartwright, D. J., "Compendium of Stress Intensity Factors," Her Majesty's Stationary Office, 1976.

[7]Newman, J. C., Jr., "Predicting Failure of Specimens with Either Surface Cracks or Corner Cracks at Holes," NASA TN D-8244, June 1976.